Flash Photolysis Studies of the Ruthenium(II) Porphyrins Ru(P)(NO)(ONO). Multiple Pathways Involving Reactions of Intermediates with Nitric Oxide[1]

Ivan M. Lorković,[†] Katrina M. Miranda,*[,†] Brian Lee,[†] Stefan Bernhard,[‡] Jon R. Schoonover,[‡] and Peter C. Ford*[,†]

Contribution from the Department of Chemistry, University of California, Santa Barbara, California 93106, and Bioscience/Biotechnology Group (CST-4), Chemical Science and Technology Division, Los Alamos National Laboratory, Los Alamos, New Mexico 87545

Received June 1, 1998

Abstract: Described are the spectra and kinetics of transients formed by laser flash photolysis of the ruthenium nitrosyl nitrito complexes Ru(P)(NO)(ONO), P = TPP (*meso*-tetraphenylporphyrin), OEP (octaethylporphyrin), TmTP (tetra(*m*-tolyl)porphyrin), and FTTP (tetra(*m*-trifluoromethylphenyl)porphyrin) in benzene solutions. Two transient decay processes are seen on the time frame (<1 ms) of the flash photolysis experiment, and a residual difference spectrum, which decays to baseline on a longer time frame, is noted as well. The accumulated evidence points to the formation of two primary photoproducts, Ru(P)(ONO) (**A**) formed by NO photolabilization and Ru(P)(NO) (**B**) formed by NO_2 photolabilization. Both decay by NO dependent pathways, the reaction of **A** with NO to re-form Ru(P)(NO)(ONO) being substantially faster ($2.4-5.5 \times 10^8$ M^{-1} s^{-1} in ambient temperature benzene) than the reaction of **B** with NO ($2.4-10 \times 10^7$ M^{-1} s^{-1}). The product of the latter reaction is apparently the dinitrosyl complex Ru(P)$(NO)_2$, which undergoes a much slower thermal reaction with excess NO to give again Ru(P)(NO)(ONO). The possibility of **B** being the oxo complex O═Ru(P)(NO) formed by NO loss from coordinated nitrite was considered but concluded to be a minor pathway at best. Isotopic exchange reactions using either labeled complex or labeled NO in cyclohexane demonstrate photochemical exchange of NO into both the nitrosyl and nitrito complexes, and time-resolved infrared experiments are consistent with formation of a long-lived nitrosyl-containing intermediate. Flash photolysis studies of the respective nitrosyl chloro complexes Ru(TPP)(NO)Cl and Ru(OEP)(NO)Cl indicate that only a single transient species, presumably Ru(P)Cl, is formed in each case, and this decays by a single NO dependent pathway back to starting material.

Introduction

Nitric oxide serves important roles in mammalian bioregulation of functions such as vasodilation, bronchodilation, and neurotransmission and also in immune response to infection.[2] These recent discoveries have stimulated interest in the chemistry and biochemistry of NO and of precursor compounds which can serve to deliver NO to biological targets on demand.[3] One strategy for NO delivery would be to employ a compound that has relatively low thermal reactivity but is photochemically active to give NO when subjected to electronic excitation. This proposition has stimulated investigations in this laboratory into the thermal and photochemical reactivities of different types of metal nitrosyl complexes,[4−9] including certain nitrosyl metalloporphyrins. Notably, metalloporphyrin and heme protein nitrosyl complexes were the subjects of photochemical studies even preceding the discovery of NO's bioregulatory functions.[10]

In the course of the present studies, it was found that nitrosyl porphyrin complexes of the first row transition metals prepared

[†] University of California.

[‡] Los Alamos National Laboratory.

(1) (a) Taken in part from the Ph.D. Dissertation of K. Miranda, University of California, Santa Barbara, 1996. (b) Taken in part from the Ph.D. Dissertation of B. Lee, University of California, Santa Barbara, 1997. (c) Reported in part at the 211th ACS National Meeting, New Orleans, March 1996, INORG 626.

(2) (a) Palmer, R. M. J.; Ferrige, A. G.; Moncada, S. *Nature* **1987**, *327*, 524−526. (b) Ignarro, L. J.; Buga, G. M.; Wood, K. S.; Byrns, R. E.; Chaudhuri, G. *Proc. Natl. Acad. Sci. U.S.A.* **1987**, *84*, 9265−9269. (c) Hibbs, J. B., Jr.; Taintor, R. R.; Vavrin, Z. *Science* **1987**, *235*, 473−476. (d) Furchgott, R. F.; Vanhoute, P. M. *FASEB J.* **1989**, *3*, 2007−2018. (e) Moncada, S.; Palmer, R. M. J.; Higgs, E. A. *Pharmacol. Rev.* **1991**, *43*, 109−142. (f) Feldman, P. L.; Griffith, O. W.; Stuehr, D. J. *Chem. Eng. News* **1993**, *71*, 10, 26−38. (g) Wink, D. A.; Hanbauer, I.; Grisham, M. B.; Laval, F.; Nims, R. W.; Laval, J.; Cook, J.; Pacelli, R.; Liebmann, J.; Krishna, M.; Ford, P. C.; Mitchell, J. B. *Curr. Top. Cell. Regul.* **1996**, *34*, 159−187. (h) Feelisch, M., Stamler, J. S., Eds. *Methods in Nitric Oxide Research*; John Wiley and Sons: Chichester, England, 1996; see also references therein.

(3) Feelisch, M.; Stamler, J. S. Ch. 7 in ref 2h, pp 71−113.

(4) Hoshino, M.; Ozawa, K.; Seki, H.; Ford, P. C. *J. Am. Chem. Soc.* **1993**, *115*, 9568−9575.

(5) Tran, D.; Ford, P. C. *Inorg. Chem.* **1996**, *35*, 2411−2412. (b) Tran, D.; Skelton, B. W., White, A. H., Laverman, L. E.; Ford, P. C. *Inorg. Chem.* **1998**, *37*, 2505−2511.

(6) Hoshino, M.; Maeda, M.; Konishi, R.; Seki, H.; Ford, P. C. *J. Am. Chem. Soc.* **1996**, *118*, 5702−5707.

(7) Bourassa, J.; DeGraff, W.; Kudo, S.; Wink, D. A.; Mitchell, J. B.; Ford, P. C. *J. Am. Chem. Soc.* **1997**, *119*, 2853−2860.

(8) Laverman, L. E..; Hoshino, M.; Ford, P. C. *J. Am. Chem. Soc.* **1997**, *119*, 12663−12664.

(9) Ford, P. C.; Bourassa, J.; Miranda, K.; Lee, B.; Lorković, I.; Boggs, S.; Kudo, S.; Laverman, L *Coord. Chem. Rev.* **1998**, *171*, 185−202.

(10) For examples: (a) Tamura, M.; Kobayashi, K.; Hayashi, K. *FEBS Lett.* **1978,** *88*, 124−126. (b) Rose, E. J.; Hoffman, B. *J. Am. Chem. Soc.* **1983**, *105*, 2866−2873. (c) Cornelius, P. A.; Hochstrasser, R. M.; Steele, A. W. *J. Mol. Biol.* **1983**, *163*, 119−128. (d) Jongeward, K. A.; Magde, D.; Taube, D. J.; Marsters, J. C.; Traylor, T. G.; Sharma, V. S. *J. Am. Chem. Soc.* **1988**, *110*, 380−387.

10.1021/ja981907o CCC: $15.00
Published on Web 11/03/1998

in this laboratory[1a] were too labile, too reactive with dioxygen, or both to be promising for practical applications in photochemical NO delivery to specific targets in biological organisms. As a consequence, attention turned to the preparation of ruthenium analogues that were anticipated to be more stable. In this context, an earlier report from this laboratory describes the synthesis, spectroscopic characterizations, and structures of several nitrosyl ruthenium complexes of tetraphenylporphyrin (TPP) and octaethylporphyrin (OEP).[11] In that report, it was noted that the principal product of the nitric oxide reaction with Ru(P)(CO) in noncoordinating solvents is the nitrosyl nitrito complex Ru(P)(NO)(ONO). Described here are the photochemical properties of such nitrosyl nitrito complexes and related species as studied by several techniques including flash photolysis with time-resolved optical (TRO) and time-resolved infrared (TRIR) spectral detection.

Experimental Section

Materials and Procedures. Prior to use in synthesis or photolysis, reagent grade benzene (dried over CaH_2), 1,2-dichloroethane (P_2O_5), dichloromethane (CaH_2), methylcyclohexane (CaH_2), cyclohexane (CaH_2), and toluene (CaH_2) were distilled under N_2. Methylcyclohexane-d_{14} was obtained from Aldrich and used as received. Chromatographic grade argon (Air Liquide) was passed through an indicating oxygen trap (Chromatograph Research Supplies). Nitric oxide (>99%; Matheson) was passed through a stainless steel column filled with Ascarite II (NaOH on a silicate carrier; Thomas Scientific) to remove higher nitrogen oxides. All manipulations of NO gas and NO-containing solutions were carried out in stainless steel or glass vessels and lines with greaseless fittings. Ruthenium dodecacarbonyl (Strem Chemicals), *meso*-tetra(*m*-tolyl)porphyrin (TmTP; Midcentury, Posen, IL), and *meso*-tetra(*m*-trifluoromethylphenyl)porphyrin (FTTP; Midcentury) were used as received.

The ruthenium nitrosyl porphyrins Ru(TPP)(NO)(ONO) (**1**), Ru(TPP)(NO)(OH), Ru(OEP)(NO)(ONO) (**2**), Ru(OEP)(NO)(OH), and Ru(TmTP)(NO)(ONO) (**3**) were prepared by the reactions of Ru(P)(CO) (P = TPP, TmTP, or OEP) with NO as described elsewhere.[1a,11] The chloro complexes Ru(TPP)(NO)Cl and Ru(OEP)(NO)Cl[12] were prepared from the hydroxyl analogues Ru(P)(NO)(OH) in CH_2Cl_2 by treatment with gaseous HCl in CH_2Cl_2 following the procedure of Bohle.[13]

Synthesis of Ru(FTTP)(NO)(ONO) (4). The carbonyl compound Ru(FTTP)(CO) was prepared from $Ru_3(CO)_{12}$ and H_2FTTP as described for Ru(TmTP)(CO).[11b,14] Upon heating on the rotary evaporator, the solution containing Ru(FTTP)(CO) darkened, and ^{1}H NMR showed the formation of a paramagnetic species (broad peaks, fwhm = 50 Hz). Chromatography on silica starting with 50/50 CH_2Cl_2/pentane and increasing the CH_2Cl_2/pentane ratio, followed by solvent removal at room temperature or lower, removed these impurities.[15] Reaction of Ru(FTTP)(CO) with NO followed by the isolation procedures described elsewhere for the TmTP analog[11b] gave two products identified spectroscopically as Ru(FTTP)(NO)(ONO) and Ru(TmTP)(NO)(OH). Spectral data for **4**: UV/visible in CH_2Cl_2 (λ_{max}, nm (ϵ, M^{-1} cm^{-1})) 409 (1.69×10^5, Soret), 559 (1.33×10^4), 600^{sh}; IR (cyclohexane, cm^{-1} (ϵ, M^{-1} cm^{-1})) 1847 (3400, ν_{NO}), 1535 (1070, $\nu_{(as)ONO}$), 1350, 1305, 1175, 1165, 1135 (2000−5000, CF_3); ^{1}H NMR ($CDCl_3$, δ vs TMS, ppm) 8.98 (8H, m, β-pyrrole), 8.39−8.56 (8H, m, *ortho*), 8.13 (4H, d, J = 8 Hz, *meta*), 7.96 (4H, m, J = 8 Hz, *para*); FAB-MS (*m*/*z*, relative intensity, assignment) (expected MW of Ru(FTTP)(NO)(ONO) = 1062) 1063 (<1, Ru(FTTP)(NO)(ONO) + H^+), 1033 (10, Ru(FTTP)-(NO)(ONO) − NO + H^+), 1016 (100, Ru(FTTP)$(NO)^+$), 1002 (25, Ru(FTTP)$(O)^+$), 986 (50, Ru(FTTP)$^+$).

Instrumentation. Electronic absorption spectra were measured in 0.0202 cm CaF_2 and 0.2 and 1 cm quartz cells on Hewlett-Packard 8452A diode array and Cary 118 (OLIS digital upgrade) spectrophotometers. Infrared spectra of solid samples in a KBr matrix and of dichloromethane or cyclohexane solutions were recorded with a Bio-Rad FTS-60 FTIR spectrophotometer. NMR spectra were obtained on Varian 200, 400, and 500 MHz spectrometers in $CDCl_3$ ($CHCl_3$ at 7.260 ppm). FAB mass spectra (xenon atom bombardment of a 3-nitrobenzyl alcohol matrix) were obtained on a VG 70E double focusing mass spectrometer.

Photolysis Solutions. Solutions for photolysis experiments were prepared with optical densities of ~0.6 (10^{-5}−10^{-6} M) at the monitoring wavelength. If necessary, mild sonication was used to facilitate dissolution. Solutions were protected from room light with aluminum foil and used within an hour of preparation. When stored in the dark, solid samples of Ru(P)(NO)(OH) proved to be stable in air for months; however, under identical conditions, Ru(P)(NO)(ONO) slowly degraded to Ru(P)(NO)(OH). To remove this impurity, the Ru(P)(NO)(ONO) was dissolved in dichloromethane and passed through a Pasteur pipet filled with Al_2O_3/CH_2Cl_2 (activity grade 1; Merck) immediately before preparation of photolysis solutions. The column elutant containing Ru(P)(NO)(ONO) was collected in a round-bottom flask while Ru(P)(NO)(OH) remained on the column. The solvent was immediately removed under vacuum, and photolysis solutions were prepared in the desired solvent. An alternative way of preparing such solutions was to dissolve the Ru(P)(NO)(ONO) solid containing some Ru(P)(NO)(OR) impurity under a NO atmosphere and then allow it to react with N_2O_3 (generated by introducing a small amount of O_2), a procedure which converts the latter cleanly to Ru(P)(NO)(ONO).

Photolysis solutions (5−10 mL) were deaerated by the freeze−pump−thaw (f−p−t) method in a laser photolysis cell (total volume 60 mL) that consisted of a triple O-ring Chemglass Teflon stopcock, a four-sided quartz cuvette, and an O-ring adapter for connection to a gas/vacuum manifold. Typically, four f−p−t cycles were sufficient to remove the dissolved gases. After degassing, the sample cell was opened to the manifold to equilibrate with a barometric measured pressure of NO or Ar. The concentrations of NO were calculated from the P_{NO} and the known solubility of NO in benzene.[16] The electronic absorption spectra of photolysis solutions were recorded on a Hewlett-Packard 8452A diode array spectrophotometer immediately before and after laser flash photolysis to determine the degree of sample decomposition.

Laser Flash Photolysis Instrumentation. Two systems were used for time-resolved optical (TRO) absorption observation. The first employed a photomultiplier tube (PMT) detector to obtain kinetic traces at a single observation wavelength.[17] TRO spectra were recorded point by point by using a monochromator in the optical train to vary the observation wavelength. The second system used a CCD camera to record transient spectra at specified delay times.[18] The pump source for all UV/visible transient absorption work was the frequency-doubled

(11) (a) Miranda, K. M.; Bu, X.; Lorković, I.; Ford, P. C. *Inorg. Chem.* **1997**, *36*, 4838−4848. (b) Lorković, I.; Ford, P. C. Submitted for publication.

(12) Spectroscopic data for Ru(OEP)(NO)Cl: UV/visible (CH_2Cl_2, λ_{max} ($\epsilon/10^3$, M^{-1} cm^{-1})): 354 nm (31), 399 (140, Soret), 467^{sh} (8.8) 547^{sh} (6.6), 568 (6.8); IR (CH_2Cl_2, KBr): 1844 (1300 $M^{-1}cm^{-1}$), 1827 cm^{-1}; ^{1}H NMR ($CDCl_3$, δ): 10.39 ppm (s, 4H, meso), 4.19 (m, diastereotopic CH_2CH$_3$, 16H, J = 7.5 Hz), 2.01 (t, CH$_2$CH_3, 24H, J = 7.5 Hz); FAB-MS 699 *m*/*z* (parent), 669 (Ru(OEP)$(Cl)^+$), 664 (Ru(OEP)$(NO)^+$), 634 (Ru(OEP)$^+$). Spectroscopic data for Ru(TPP)(NO)Cl: H NMR ($CDCl_3$, δ) 9.01 ppm (s, 8H, β-pyrrole), 8.89 (m, 8H, *meta*), 4.98 (m, 12H, *ortho*, *para*); UV/visible (benzene, λ_{max} ($\epsilon/10^3$, M^{-1} cm^{-1})) 332 nm (21); 414 (Soret, 180), 564 (9), 610 (sh, 3.5).

(13) (a) Bohle, D. S.; Goodson, P. A.; Smith, B. D. *Polyhedron* **1996**, *15*, 3147−3150. (b) Massoudipour, M.; Pandey, K. K. *Inorg. Chim. Acta* **1989**, *160*, 115−118.

(14) Barley, M.; Becker, J. Y.; Domazetis, G.; Dolphin, D.; James, B. R. *Can. J. Chem.* **1983**, *61*, 2389−2396.

(15) (a) ^{1}H NMR spectral data for Ru(FTmTP)(CO): ^{1}H NMR, $CDCl_3$, δ vs TMS 8.66 (8H, m), 8.40 (b m, 8H), 8.06 (4H, d, J = 7.6 Hz), 7.89 (4H, t, J = 7.6 Hz). (b) The ^{1}H NMR spectrum of Ru(FTTP)(NO)(ONO) is more complex than that of Ru(FTTP)(CO) or of **3**,[11b] but in $CHCl_3$ coalescence to a higher symmetry spectrum is observed at temperatures approaching 60 °C. This behavior suggests atropisomer interconversion (by tolyl rotation) with lifetimes on the order of seconds at room temperature for **4** in $CDCl_3$.

(16) Oxides of Nitrogen. In *IUAPC Solubility Data Series*; Young, C. L., Ed.; Pergamon Press: Oxford, 1983; Vol. 8.

(17) Crane, D. R.; Ford, P. C. *J. Am. Chem. Soc.* **1991**, *113*, 8510−8516.

(18) Lindsay, E.; Ford, P. C. *Inorg. Chim. Acta* **1996**, *242*, 51−56.

(532 nm) or -tripled (355 nm) output of a Continuum NY-61 Nd:YAG pulsed laser with harmonic generators. The power was attenuated to approximately 20 mJ/pulse. For kinetic traces and point by point transient spectra, the probe beam was the output from an ILC Technology R300-5 300 W xenon lamp passed through an IR filter and a high-throughput monochromator. The probe and pump beams were approximately collinear, so the probe was passed through a SPEX Model 1680 Doublemate grating monochromator before detection at the RCA 8852 PMT. The output of the PMT was recorded by a Tektronix TDS 540 digital oscilloscope and transferred to a computer for data analysis and storage. For CCD experiments, the probe beam was output from an Osram Xenophot HLX lamp set perpendicular to the excitation beam. This was focused onto the sample, collected, refocused onto a fiber optic, and brought to a SpectraPro-275 triple grating monochromator from Acton Research Corp. The probe light was then gated by a MCP intensifier, which was run from a PG-200 programmable pulse generator from Princeton Instruments, Inc. The gated light was imaged onto a liquid nitrogen cooled, Princeton Instruments Model 1024-EUV CCD from which data were transferred to a computer.

Data Analysis. Intensity vs time traces obtained by single wavelength detection were converted to ΔAbs vs time plots by use of either ScopeMate (a custom program by UGI Scientific) or Igor (Wavemetrics) software. Curve fitting of ΔAbs vs time traces was accomplished using Kaleidagraph or Igor while point by point spectra were generated using Igor or Sigma Plot. Rate constants for first-order reactions were determined by fitting the data to the equation for an exponential curve. Two other computational models were also used. For two parallel first-order reactions leading to a common product

$$A \xrightarrow{k_1} C \tag{1}$$

$$B \xrightarrow{k_2} C \tag{2}$$

the rate constants, k_1 and k_2, were obtained from the curve fit to eq 3 (a and b = amplitude of the first and the second exponential curves,

$$\Delta\text{Abs} = ae^{-k_1 t} + be^{-k_2 t} + c \tag{3}$$

respectively; c = Abs at $t = \infty$). For a serial pair of "first order" reactions

$$A \xrightarrow{k_1} B \xrightarrow{k_2} C \tag{4}$$

the rate constants, k_1 and k_2, were obtained from the curve fit to eq 5 (A_0 = [A] at $t = 0$; ϵ_X = extinction coefficient of X; c = Abs at $t = \infty$).

$$\Delta A = [(\epsilon_B - \epsilon_C)(A_0 k_1)(e^{-k_2 t} - e^{-k_1 t})/(k_2 - k_1)] + (\epsilon_A - \epsilon_C)(A_0 e^{-k_1 t}) + c \tag{5}$$

Second-order rate constants for reaction with NO were obtained from the slopes of k_i vs [NO] plots. Unless otherwise stated, experimental uncertainties in the second-order rate constants, estimated conservatively from the reproducibilities of the k_i values extracted from numerical analyses of biexponential curves and these plots, were about ±20%.

Isotope Labeling Experiments. Isotopically labeled nitric oxide $^{15}N^{18}O$ was purchased from Isotec Inc. and used without further purification. Saturated methylcyclohexane-d_{14} solutions of Ru(TmTP)(NO)(ONO) (~1 mL, ~1.4 mM) were prepared in a flask of known volume (30 mL) with an airless Teflon stopcock and a port sealed with a rubber/silicone/rubber septum. After the solution was degassed by several f−p−t cycles, a known amount of $^{15}N^{18}O$ (about 0.3 atm at 298 K, to make a 5 mM solution of $^{15}N^{18}O$) was condensed into the flask. From this point on, the solution was kept in the dark except when intentionally irradiated. After thawing, the flask was brought into an argon-filled glovebox, and the inlet valve quickly opened and shut for pressure equilibration. The solution was swirled to equilibrate the vapor and liquid. An aliquot of the solution was then transferred by syringe (through the septum) into an IR cell with CaF_2 windows and a 1.0 mm path length which was quickly sealed with Teflon stoppers. Enough solution (~0.4 mL) was used to minimize headspace in the IR cell. After an initial spectrum was taken, the sample was allowed to sit in the dark for 30 min, and another spectrum was recorded to determine the degree of nonphotochemical ligand exchange. Thereafter, the sample was irradiated for 30 s intervals with a hand-held UV lamp, operating in long-wavelength mode (mostly 365 nm), held directly above the cell window (2.5 cm). After each irradiation interval, FTIR spectra were recorded. The initial spectrum was then digitally subtracted from the subsequent spectra to show consumption of starting material and growth of photoproduct. Analogous experiments were carried out using fully labeled Ru(TmTP)($^{15}N^{18}O$)($^{18}O^{15}N^{18}O$) (prepared from the reaction of Ru(TmTP)(CO) with $^{15}N^{18}O$) and unlabeled NO.

Table 1. Electronic Spectra of Ru(P)(NO)(X) Compounds in Ambient Temperature CH_2Cl_2

	λ_{max}, nm (log ϵ, M^{-1} cm^{-1})		
compound	Soret band	Q(1,0)	Q(0,0)
Ru(TPP)(NO)(ONO) (**1**)	410 (5.32)	564 (4.01)	608^{sh}(3.65)
Ru(OEP)(NO)(ONO) (**2**)	396 (5.15)	546^{sh}(3.83)	574 (3.87)
Ru(TmTP)(NO)(ONO) (**3**)	411 (5.30)	561 (4.01)	606^{sh}
Ru(FTTP)(NO)(ONO) (**4**)	409 (5.23)	559 (4.12)	600^{sh}
Ru(OEP)(NO)Cl	399 (5.15)	547^{sh} (3.82)	568 (3.83).
Ru(TPP)(NO)Cl	414 (5.26)	564 (3.95),	610^{sh} (3.54)

Step-Scan FTIR Experiments. These were carried out on flowing room-temperature cyclohexane solutions of Ru(TmTP)(NO)(ONO) with added NO (0.1−0.9 atm).[1b] The sample cell was a 2 mm path length CaF_2 IR cell. The instrument was a modified BioRad FTS 60A/896 step-scan FTIR using a photoconductive HgCdTe detector (Graseby 1710117) at Los Alamos National Laboratory.[19] The IR signal from the detector was amplified (Graseby DP-8000-4 amplifier, rise time 1 μs) and processed by a BioRad Fast TRS board (200 ns time resolution) installed in a Pentium PC. The data were processed by the BioRad version of WIN-IR Pro. The third harmonic of a Nd:YAG laser was used as the photochemical excitation source (Spectra Physics DCR-11).

Results and Discussion

Spectra. The electronic spectra of compounds **1**−**4** recorded in dichloromethane are summarized in Table 1. Figure 1 displays the spectra of compounds **1** and **2**. The absorption bands observed for each of these compounds are relatively independent of solvent medium.

Observations Regarding the Photostability of Ru(P)(NO)(ONO). As noted below, the flash photolysis of these porphyrin compounds with 355 nm light in a weakly coordinating solvent such as benzene led to the formation of transient species that decay by NO dependent pathways to re-form the starting complexes. Under NO (≥100 Torr) little net photochemistry was seen as the result of multiple pulse laser excitation or continuous photolysis from a monochromatic light source or room light. However, low-yield permanent photochemistry was seen for Ru(P)(NO)(ONO) solutions under argon or vacuum or even under lower P_{NO}. The resulting photoproducts were not characterized, although optical density changes were consistent with the formation of the hydroxyl nitrosyl complexes Ru(P)(NO)(OH). Net photoreactivity was also seen when Ru(TPP)(NO)(ONO) was irradiated in the presence of pyridine, and the product was identified spectrally as the bis(pyridine) adduct Ru(TPP)$(py)_2$.[20] Similarly, the major photoproduct of Ru(P)(NO)(ONO) (P = TPP or OEP) in chlorocarbon solvents was characterized spectrally (IR, NMR) as Ru(P)(NO)Cl.[12]

Laser Flash Photolysis Studies. Flash photolysis experiments were carried out under various NO partial pressures using

(19) Schoonover, J. R.; Strouse, G. F.; Omberg, K. M.; Dyer, R. B. *Comments Inorg. Chem.* **1996**, *18*, 165−188.
(20) Chow, B. C.; Cohen, I. A. *Bioinorg. Chem.* **1971**, *1*, 57−63.

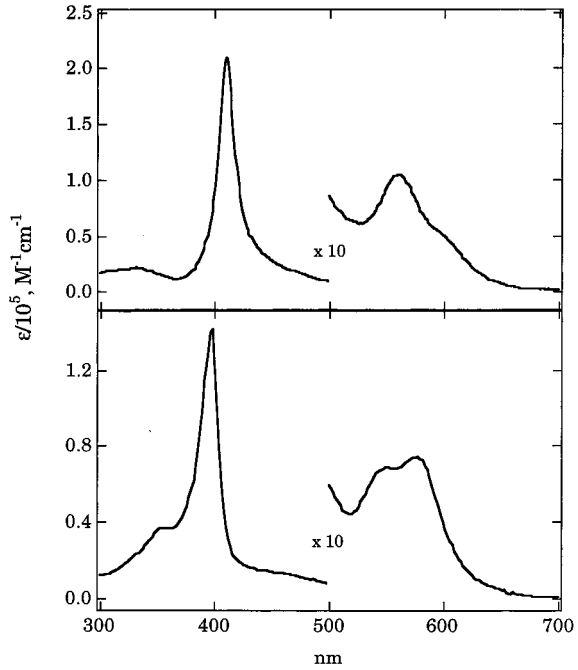

Figure 1. Room-temperature UV/visible absorption spectra in CH_2Cl_2. Top: Ru(TPP)(NO)(ONO) (**1**). Bottom: Ru(OEP)(NO)(ONO) (**2**).

355 nm. (Attempts to use 532 nm excitation were frustrated by the very low photoreactivity of the nitrosyl nitrito complexes **1**−**4** at that wavelength.) The TRO spectral properties of the four substrates demonstrated consistent behavior. Absorption bands characteristic of the parent complexes were promptly (within the 10 ns width of the excitation) bleached, and new, transient absorptions in the Soret and Q-band regions were immediately evident. In the Q-band region, where bands of individual species are broader and overlap considerably, the decay kinetics of both transient absorptions and transient bleaches indicated multiple processes and required numerical analysis by multiexponential functions at each monitoring wavelength λ_{mon}. In the (narrower) Soret band region, the transient absorption decays tended to be more consistent with single exponential functions, although this generally did not hold true for the recovery of the bleached band of the parent. Furthermore, while the flash induced absorbance changes of Ru(P)(NO)(ONO) solutions under NO decayed to values close to zero (i.e., to the original spectrum) within 100 μs, residual changes did persist. This was particularly evident at the λ_{mon} corresponding to the substrate Soret band λ_{max}, but even these changes largely decayed back to baseline on a substantially longer (millisecond to second) time frame.

Ru(TPP)(NO)(ONO) (1). Pulsed laser excitation at 355 nm with single wavelength (PMT) detection at various λ_{mon} demonstrated immediate (<10 ns) ground-state bleaching in the Q-band region with the most negative ΔAbs at 558 nm (near the Q(1,0) band λ_{max} at 562 nm for **1**). A corresponding transient absorption with λ_{max} of 528 nm was also observed. Typical ΔAbs vs time profiles at 465 nm (transient bleach) and at 525 nm (transient absorption) are shown in Figure 2. These and related data regarding temporal Q-band absorbances could not be fit satisfactorily to single exponential decays. The data did, however, give good mathematical fits (correlation constants >0.997) for a model involving two parallel exponential decays with different rate constants (k_1 and k_2) (Figure 2). The k_1 and k_2 represent the decays of two photoproduct intermediates generated within the time scale of the laser flash, leading to the same product (A → C and B → C, where C is **1**) or, possibly,

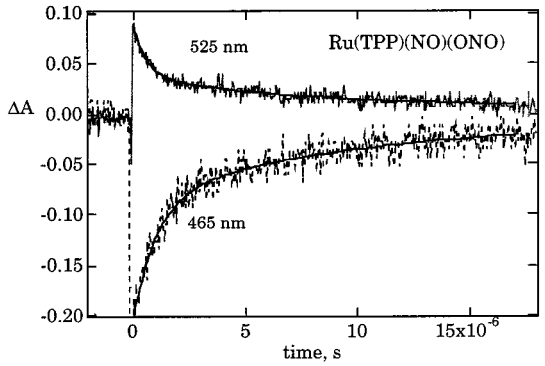

Figure 2. Decays of the transient bleaching at 465 nm and of transient absorption at 525 nm following 355 nm laser flash photolysis of a benzene solution of Ru(TPP)(NO)(ONO) under nitric oxide (4.2×10^{-3} M) ($T = 295$ K, data averaged over ~60 pulses)). The fit shown is for a model based on two parallel first-order processes (A → C, B → C) as described in the text.

Scheme 1

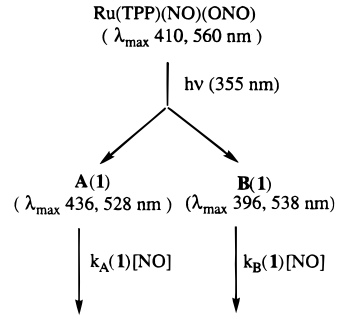

two different products of closely similar spectra. An alternative mechanism based on sequential exponential decays from a single primary photoproduct (A → B → C) gave numerical fits of comparable quality; however, transient spectral changes support the prompt formation of two species. Furthermore, the mechanistic implication of the latter scenario, i.e., two ligands labilized by single photon excitation, is less likely. For this reason, analysis according to simultaneous decay of two promptly formed intermediates (Scheme 1) will be used in the subsequent discussion.

When benzene solutions of **1** were subjected to flash photolysis under different P_{NO}, analysis of the subsequent temporal spectral changes in the Q-bands demonstrated both components of the decay kinetics to be dependent on [NO]. Linear plots of the observed rate constants, k_1 and k_2 (determined at 558 nm), vs [NO] (1−10 mM) are shown in Figure 3. The second-order rate constants obtained from their slopes are $k_A(\mathbf{1}) = 2.5 \times 10^8\ M^{-1}\ s^{-1}$ and $k_B(\mathbf{1}) = 2.8 \times 10^7\ M^{-1}\ s^{-1}$ (where the subscripts A and B refer to the first (faster) and second (slower) processes, respectively, and the (**1**) indicates the compound under consideration).

The decay of the transient absorption at 528 nm was also analyzed in terms of the same model to give the observed rate constants k_1 and k_2. Plots of these k_{obs} values vs [NO] were also linear and gave the second-order rate constants 1.9×10^8 and $2.7 \times 10^7\ M^{-1}\ s^{-1}$ for $k_A(\mathbf{1})$ and $k_B(\mathbf{1})$, respectively, comparable to those determined at 558 nm.

The formation of at least two transients in the flash photolysis of **1** in benzene ([NO] = 9.6×10^{-3} M) was confirmed by the time-resolved optical (TRO) spectra in the Q-band region recorded with a CCD camera. Figure 4 illustrates the spectra collected shortly after the flash (100 ns) and after delays of 2

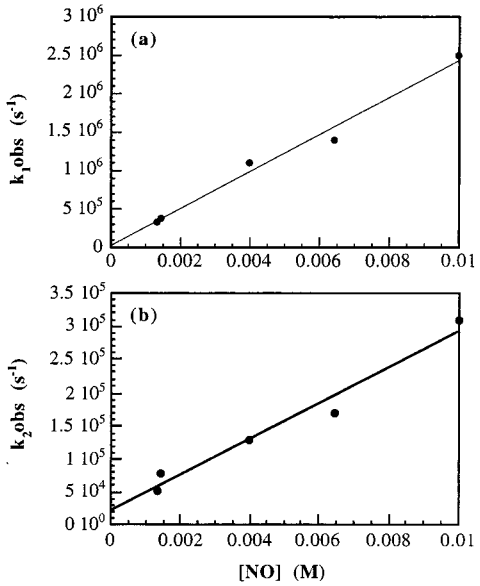

Figure 3. k_1 (a) and k_2 (b) vs [NO] for the decay of the transient bleaching (558 nm) of Ru(TPP)(NO)(ONO) after laser flash photolysis at 355 nm in benzene: $k_A(\mathbf{1}) = 2.5 \times 10^8$ M^{-1} s^{-1} and $k_B(\mathbf{2}) = 2.8 \times 10^7$ M^{-1} s^{-1}. (The parallel decay model (A → C, B → C) was used to calculate the k_{obs} values.)

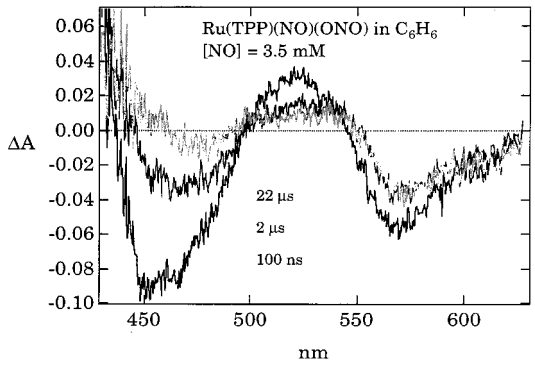

Figure 4. Transient absorption difference spectra in the Q-band region for Ru(TPP)(NO)(ONO) after laser flash photolysis at 355 nm in benzene.

and 22 μs. The prompt spectral change is described by a bleach centered at 455 nm, a positive peak at 528 nm, and a bleach at 565 nm. After 2 μs (sufficient time for the fast [NO] dependent process to be largely completed under these conditions), the difference spectrum is characterized by the disappearance of much of the bleach at ~460 nm (shoulder of Soret band), a shift in the λ_{max} of the transient absorption to 538 nm, and modest recovery of the bleach at 565 nm. After 22 μs delay (sufficient time for the second NO dependent decay to be largely completed), a significant residual spectral change remains, indicating the presence of at least a third longer lived species. This residual difference spectrum eventually returns to baseline over a much longer period (seconds).

Flash photolysis of **1** using single wavelength detection in the Soret region demonstrated prompt transient bleaching with the largest ΔAbs at 412 nm (as compared to the Soret band λ_{max} of 410 nm for **1**) and in smaller transient absorbances (about 20% of the ΔAbs at 412 nm) with ΔAbs maxima at 396 and 436 nm. In contrast to the Q-band region, some individual traces collected in the Soret region could be analyzed as single exponential decays. The ΔAbs at 396 nm decayed at a much slower rate (k_2) than that at 436 nm (k_1), indicating that the former wavelength is sampling (principally) the longer lived

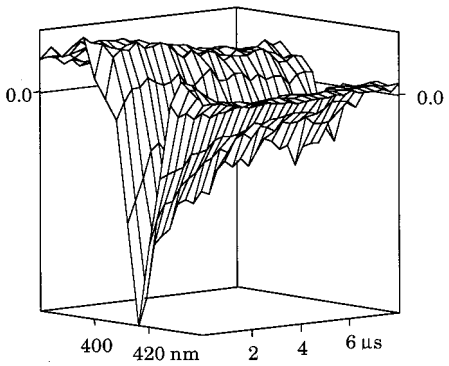

Figure 5. Stack plot of temporal spectra in the Soret region after 355 nm laser flash photolysis of Ru(TPP)(NO)(ONO) in benzene ([NO] = 3.5×10^{-3} M).

intermediate while the latter is sampling the shorter lived intermediate. The return of the Soret absorbance at 412 nm proved to be predominantly due to the faster decay process, since the amplitude attributable to the slower component (although evident) was too small to give a reliable numerical analysis. In addition, the decays of the transient absorbances at 396 and 436 nm and of the Soret band bleach at 412 nm each proved to be dependent on [NO]. Linear plots of k_{obs} values vs [NO] gave the second-order rate constants 2.8×10^8 M^{-1} s^{-1} at 412 nm, 2.9×10^8 M^{-1} s^{-1} at 436 nm, and 2.0×10^7 M^{-1} s^{-1} at 396 nm. The first two values are consistent with the $k_A(\mathbf{1})$ measured in the Q-band region, while the third is in agreement with the $k_B(\mathbf{1})$ thus determined. TRO spectra recorded in the Soret region using the CCD camera agreed well with those obtained by using the point by point method (Figure 5).

The dual pathway kinetics, observable at the Q(1,0) maximum but not reliably at the Soret maximum, were reproduced by single wavelength monitoring at the edge of the Soret band (465 nm) where transient bleaching was observed with complete return to baseline. At this λ_{mon}, the value of $k_A(\mathbf{1})$ (from k_1 vs [NO]) was determined to be 2.0×10^8 M^{-1} s^{-1} while that of $k_B(\mathbf{1})$ (from k_2 vs [NO]) equaled 2.3×10^7 M^{-1} s^{-1}. Thus, numerical analysis of temporal absorbance changes in both the Soret and Q-band regions gave consistent rate constant values for the two decay processes ($(2.4 \pm 0.5) \times 10^8$ and $(2.4 \pm 0.4) \times 10^7$ M^{-1} s^{-1}).

Ru(OEP)(NO)(ONO) (2). Pulsed laser excitation (355 nm) of a benzene solution of **2** with broad band (CCD) detection gave prompt transient bleaching with minima at 400, 470, and 585 nm (the first and third corresponding roughly to the Soret and Q-band λ_{max} for **2**) and transient absorptions with maxima at 380, 423, and 530 nm. Similar to the TPP analogue, the traces collected by single wavelength detection in the Soret region are primarily composed of simple decays with k_{obs} values linearly dependent on [NO]. The return of the Soret band at 400 nm appeared to be predominantly due to decay of the fast intermediate; a second, slower component had a much smaller amplitude and did not give a reliable numerical analysis for k_2. The disappearance of the transient ΔAbs at 423 nm also followed the faster process and gave $k_A(\mathbf{2}) = 3.6 \times 10^8$ M^{-1} s^{-1} with little contribution from the $k_B(\mathbf{2})$ pathway. In contrast, the transient ΔAbs at 380 nm decayed at a much slower rate, also linearly dependent on [NO], giving $k_B(\mathbf{2}) = 1.0 \times 10^8$ M^{-1} s^{-1}. In the Q-band region, decay of transient bleaching ($\lambda_{max} \approx 590$ nm) and of transient absorption ($\lambda_{max} \approx 530$ nm) required numerical analysis in terms of a two-component model. Fits

of temporal absorbance changes at 533 nm gave the fast and slow components, and plots of k_1 and k_2 vs [NO] gave k_A(**2**) (4.0×10^8 M^{-1} s^{-1}) and k_B(**2**) (1.0×10^8 M^{-1} s^{-1}). These are consistent with rates recorded for decays of transient absorbances at 423 and 380 nm, respectively.

Ru(TmTP)(NO)(ONO) (3). Pulsed laser excitation of a benzene solution of **3** with broad band detection generated a prompt difference spectrum with a Soret band bleach at 412 nm and absorptions at 395 and 435 nm. The decay of transient bleaching and return to baseline of transient absorbances were followed using single wavelength detection and could be analyzed as exponential decays. However, the k_{obs} values determined at 435 nm were about an order of magnitude faster than at 395 nm under identical conditions. Furthermore, dynamic behavior at 412 nm was closer to that at 435 nm, again showing that, while double exponential decay might have been expected, the amplitude for the faster process was larger. Plots of k_{obs} vs [NO] gave second-order rate constants of k_A(**3**) = 5.5×10^8 M^{-1} s^{-1} at 435 nm and k_B(**3**) = 4.7×10^7 M^{-1} s^{-1} at 395 nm, both slightly higher than the analogous rate constants described for the flash photolysis of **1** in benzene. At 460 nm, the parallel reaction model was needed to analyze the decay curves, and plots of k_1 and k_2 values determined in this manner vs [NO] gave the second-order rate constants k_A(**3**) = 5.5×10^8 M^{-1} s^{-1} and k_B(**3**) = 3.6×10^7 M^{-1} s^{-1}.

In the Q-band region, transient bleaching of **3** at 560 nm was accompanied by a transient absorption λ_{max} at 520. At both wavelengths the temporal data were analyzed according to the model using the parallel decays of two intermediates. Plots of the k_{obs} values vs [NO] gave the second-order rate constants k_A(**3**) = 5.5×10^8 M^{-1} s^{-1} and k_B(**3**) = 5.1×10^7 M^{-1} s^{-1} at 560 nm and 4.5×10^8 and 4.7×10^7 M^{-1} s^{-1} at 520 nm. These are in reasonable agreement with the k_A(**3**) and k_B(**3**) values determined in the Soret band region.

Ru(TmTP)(NO)(ONO) was chosen as a substrate to enhance solubility in solvents appropriate for IR studies and is moderately soluble in cyclohexane and methylcyclohexane. Notably, 355 nm flash photolysis of **3** in cyclohexane shows some qualitative differences from the results in benzene. Broad band detection showed a bleach of the Soret and Q-bands of **3** as well as transient absorption at 520 nm. Kinetic experiments with single frequency detection at 412, 450, 524, and 562 nm all gave exponential decays, and plots of k_{obs} vs [NO] (1−10 mM) gave a consistent second-order rate constant of $(9.5 \pm 1) \times 10^8$ M^{-1} s^{-1}. This is about twice that for the faster process in benzene and perhaps indicates the reactivity of a more weakly solvated intermediate in cyclohexane. The second, slower process did not appear to be present in cyclohexane; however, there was a considerable residual spectral change that persisted (>100 ms) but eventually returned to baseline (see below).

Ru(FTTP)(NO)(ONO) (4). The broad band spectrum of a benzene solution of **4** after pulsed laser 355 nm excitation was analogous to those recorded for **1** and **3**. Temporal absorbance changes (single wavelength detection) demonstrated two decay processes, although with considerable scatter in k_1 and k_2 values. Plots of k_1 vs [NO] gave k_A(**4**) of 3.1×10^8 M^{-1} s^{-1} (411 nm, transient bleaching), 4.3×10^8 M^{-1} s^{-1} (455 nm, transient absorbance), 2.4×10^8 M^{-1} s^{-1} (515 nm, absorbance), and 3.7×10^8 M^{-1} s^{-1} (555 nm, bleaching) for an average value of $(3.4 \pm 1) \times 10^8$ M^{-1} s^{-1}. Plots of k_2 vs [NO] gave the k_B(**4**) values 7.1×10^7 M^{-1} s^{-1} (455 nm), 2.5×10^7 M^{-1} s^{-1} (515 nm), and 4.2×10^7 M^{-1} s^{-1} (555 nm) for an average of $(4.6 \pm 2.5) \times 10^7$ M^{-1} s^{-1}.

Table 2. Second-Order Rate Constants Observed for the Fast and Slow Decays of Intermediates Observed in the 355 nm Laser Flash Photolysis of Ru(P)(NO)(ONO) in 296 K Benzene or Cyclohexane Solution[a]

Ru(P)(NO)(ONO)	k_A (M^{-1} s^{-1})	k_B (M^{-1} s^{-1})
Ru(TPP)(NO)(ONO)[b]	$(2.4 \pm 0.5) \times 10^8$	$(2.4 \pm 0.4) \times 10^7$
Ru(OEP)(NO)(ONO)[b]	$(3.8 \pm 0.4) \times 10^8$	$(1.0 \pm 0.1) \times 10^8$
Ru(TmTP)(NO)(ONO)[b]	$(5.5 \pm 0.6) \times 10^8$	$(4.5 \pm 0.7) \times 10^7$
Ru(TmTP)(NO)(ONO)[c]	$(9.5 \pm 1) \times 10^8$	
Ru(FTPP)(NO)(ONO)[b]	$(3.4 \pm 1.0) \times 10^8$	$(4.6 \pm 2.5) \times 10^7$
Ru(FTPP)(NO)(ONO)[c]	$(1.1 \pm 0.1) \times 10^9$	

[a] Values listed are averages of those determined at different monitoring wavelengths. [b] In benzene. [c] In cyclohexane.

The TRO spectrum of **4** in cyclohexane after 355 nm excitation showed bleaches at 455 and 560 nm and a transient absorption at 515 nm. The decays were monitored at all three wavelengths with the consistent result that, under added NO, fast single exponential decays were found which gave the second-order rate constant $(1.1 \pm 0.1) \times 10^9$ M^{-1} s^{-1}. There was also a long-lived residual absorbance that returned to baseline over a time frame longer than 50 ms.

Possible Mechanisms. In brief summary, flash photolysis (355 nm) of the Ru(P)(NO)(ONO) complexes **1**, **2**, **3**, and **4** in benzene in *each case* leads to prompt generation of two intermediates **A**(*i*) and **B**(*i*), where "*i*" denotes the precursor, i.e., **1**, **2**, **3**, or **4**. These two species decay by independent pathways, each first-order in [NO], to give a spectrum (after several hundred microseconds) similar to that of the initial nitrosyl nitrito complex but demonstrating a significant residual spectrum. Over a much longer time scale, even the residuals, initially thought to be the result of minor side reactions (see below), disappeared and the starting spectrum was fully regenerated. For each Ru(P)(NO)(ONO) **A**(*i*) displayed an apparent Soret band maximum at longer wavelength than that for the precursor while that of **B**(*i*) appeared at shorter wavelength (see Scheme 1 for **1**). Kinetic analyses of the temporal absorption changes in the Q-band region (eqs 1−3) gave k_A(*i*) and k_B(*i*) values self-consistent with those determined in the Soret band region (Table 2).

Possible identities of **A**(*i*) and **B**(*i*) include primary photoproducts, singlet or triplet excited states (ES), and π radicals resulting from charge transfer.[21] However, the relatively long lifetimes and the second-order kinetics for decay argue against these being electronic excited states. Furthermore, π,π^* ES and π radicals display strong absorptions to the red of the Q-bands, and such absorptions were not detected. Thus, **A**(*i*) and **B**(*i*) appear to be ground-state photoproducts, both formed by the loss of NO.

One model we have considered is illustrated in Scheme 2. In this, **A**(*i*) is proposed to originate from homolytic cleavage of a nitrosyl−ruthenium bond to give a ruthenium(III) nitrito complex, Ru^{III}(P)(ONO) (or the solvated analogue), and **B**(*i*) is formed by cleavage of the O−N bond of coordinated nitrite to leave an intermediate, which can be represented as O=Ru^{IV}(P)(NO) or some resonance-stabilized hybrid configuration. There is ample precedent for both pathways. NO labilization is the most common photoreaction of metalloporphyrin nitrosyl complexes;[10] e.g., both iron(II) and iron(III) porphyrin nitrosyls liberate NO upon flash photolysis followed by rapid recombination to regenerate the original complexes.[4] With regard to the second pathway, NO photolabilization from coordinated nitrite concomitant with formation of the metal−oxo species has been

(21) Kalyanasundaram, K. *Photochemistry of Polypyridine and Porphyrin Complexes*; Academic Press: London, 1992.

Scheme 2

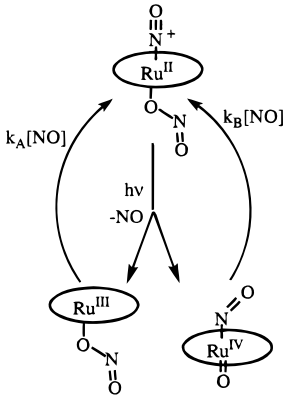

demonstrated for the chromium(III) complex Cr^{III}(TPP)(ONO) (eq 6).[22] Such a pathway has also been described as a

$$Cr^{III}(TPP)(ONO) \xrightarrow{h\nu} Cr^{IV}(TPP)(=O) \qquad (6)$$

photoreaction of the manganese(III) nitrato and nitrito complexes Mn(TPP)(NO_3) and Mn(TPP)(ONO), which were reported to give O═Mn(TPP) and NO_x products by homolytic cleavage[23] (however, see below).

TRO spectra seen in the flash photolysis of **1** can be compared with spectral data for various TPP complexes.[20,24−30] For instance, spectra of Ru^{II}(TPP) complexes with a strong π-acceptor ligand, such as NO^+ or CO, show only minor shifts (usually $\leq$5 nm) of the Soret and Q(1,0) band maxima upon changing the sixth ligand.[11a,24−26] Spectral shifts of ΔAbs λ_{max} appear much larger for both **A**(**1**) and **B**(**1**), arguing against simple photosubstitution for ONO^- to give Ru^{II}(P)(NO^+)(L) or Ru^{II}(P)(NO^+)(Sol) (Sol = solvent). On the other hand, replacement of NO^+ to give Ru^{II}(TPP)L_2 or Ru^{II}(P)$(Sol)_2$ would result in even larger hypsochromic Q-band shifts[27−29] than seen for **A**(**1**) or **B**(**1**). Similar comparisons eliminate the $[Ru^{II}(TPP)]_2$ dimer.[28,30] Thus, the spectral changes suggest that Ru^{II}(P)(NO^+)(X), Ru^{II}(P)(NO^+)(Sol), and Ru^{II}(P)$(Sol)_2$ as well as dimers are unlikely candidates for **A**(*i*) or **B**(*i*). However, one must add the caveat that difference spectra can be deceptive owing to the overlapping nature of the bands.

The flash photolysis behavior of the chloronitrosyl complex Ru(TPP)(Cl)(NO) (**5**) in benzene was briefly examined in order to model that of a ruthenium porphyrin nitrosyl in the absence of possible competing reactions of the nitrito ligand. TRO spectral techniques indicated formation of a single intermediate with λ_{max} of 442 and 532 nm which decayed cleanly to the initial baseline. The decay of this transient, presumably Ru(TPP)Cl, was exponential under excess NO, and plots of k_{obs} vs [NO] were linear over the [NO] range 1−10 mM ($k_{Cl} = (6 \pm 2) \times 10^7$ M^{-1} s^{-1}). These data are compatible with simple photodissociation of NO followed by second-order regeneration of Ru(TPP)(Cl)(NO) (eq 7). Studies with the OEP complex Ru(OEP)(Cl)(NO) gave analogous results with $k_{Cl} = (1.5 \pm 0.2) \times 10^8$ M^{-1} s^{-1}.

Scheme 3

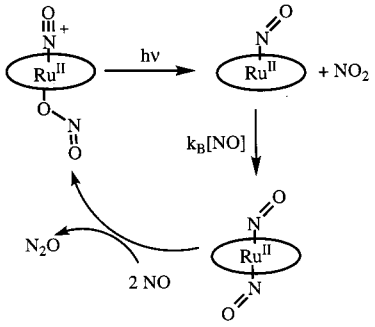

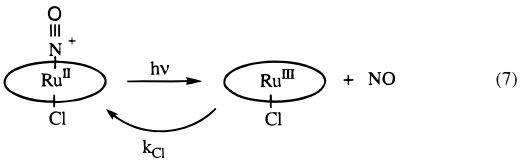

(7)

The band shifts noted on the flash photolysis of **5** are quite similar to the spectral differences between **1** and **A**(**1**). Thus, we conclude that **A**(**1**) is the Ru^{III}(TPP)(ONO) product of NO dissociation from Ru^{II}(TPP)(NO^+)(ONO) (eq 8). We also extrapolate this conclusion to the **A**(*i*) formed in the photolyses of **2**, **3**, and **4**.

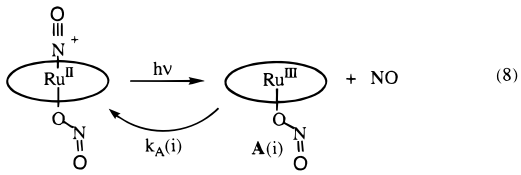

(8)

Notably, the thermal reverse reactions shown in eqs 7 and 8 are quite fast with second-order rate constants approximating 10^8 M^{-1} s^{-1}. While such rapid regeneration is often the case for other metalloporphyrins, one might expect the Ru(III) center to be hexacoordinate with a solvent molecule occupying the site previously occupied by NO. There are few quantitative studies of the reaction of NO with hexacoordinate Ru(III). One example is the reaction of NO with the normally substitution resistant hexaammine complex $Ru(NH_3)_6^{3+}$ to give $Ru(NH_3)_5(NO)^{3+}$. This apparently proceeds via an associative mechanism but is relatively slow ($k = 0.2$ M^{-1} s^{-1}).[31] In this context, we conclude that the facile reaction of NO with **A**(*i*) can be attributed to the latter being pentacoordinate or (more likely) to the high lability of Ru(P)(Sol)(ONO) (Sol in this case being benzene).[8]

Scheme 3 suggests an alternative mechanism for the formation of **B**(*i*), namely, homolytic cleavage of the Ru^{II}−(ONO^-) bond to give NO_2. This would lead to oxidation of the nitrite nitrogen from N(III) to N(IV), leaving the electron on the Ru(P)(NO) entity. If so, it is likely that the extra electron would be substantially accommodated by the nitrosyl orbitals to give a (formally) d^6 Ru^{II}(P)($NO^•$) complex with a bent Ru−NO angle

(22) Yamaji, M.; Hama, Y.; Miyazake, M.; Hoshino, M. *Inorg. Chem.* **1992,** *31*, 932−934.
(23) (a) Hoshino, M.; Iimura, Y.; Konishi, S. *J. Phys. Chem.* **1992**, *96*, 179−185. (b) Suslick, K.; Watson, R. *Inorg. Chem.* **1991**, *30*, 912−919.
(24) Levine, L. M. A.; Holten, D. *J. Phys. Chem.* **1988**, *92*, 714−720.
(25) Bonnet, J. J.; Eaton, S. S.; Eaton, G. R.; Holm, R. H.; Ibers, J. A. *J. Am. Chem. Soc.* **1973**, *95*, 2141−2149.
(26) Kadish, K. M.; Adamian, V. A.; Caemelbecke, E. V.; Tan, Z.; Tagliatesta, P.; Bianco, P.; Boschi, T.; Yi, G.-B.; Khan, M. A.; Richter-Addo, G. B. *Inorg. Chem.* **1996**, *35*, 1343−1348.
(27) Collman, J. P.; Barnes, C. E.; Brothers, P. J.; Collins, T. J.; Ozawa, T.; Gallucci, J. C.; Ibers, J. A. *J. Am. Chem. Soc.* **1984**, *106*, 5151−5163.
(28) Collman, J. P.; Barnes, C. E.; Sweptson, P. N.; Ibers, J. A. *J. Am. Chem. Soc.* **1984**, *106*, 3500−3510.
(29) Ke, M.; Sishta, C.; James, B.; Dolphin, D.; Sparapany, J. W.; Ibers. J. A. *Inorg. Chem.* **1991**, *30*, 4766−4771.
(30) Hopf, F. R.; O'Brien, T. P.; Scheidt, W. R.; Whitten, D. G. *J. Am. Chem. Soc.* **1975**, *97*, 277−281.
(31) Armor, J. N.; Scheidegger, H. A.; Taube, H. *J. Am. Chem. Soc.* **1968**, *90*, 5928−5929.

(in analogy to the known Fe(TPP)(NO) structure[32]) rather than a linear d^7 $Ru^{I}(P)(NO^{+})$ complex. Rapid reaction of Ru(P)(NO) with NO to form $Ru(P)(NO)_2$ would be followed by the much slower further reaction of the latter with NO to re-form Ru(P)(NO)(ONO)[11b] (see below). The dinitrosyl might also be reoxidized by reaction with N_2O_3, the product of the very fast reaction of NO_2 with excess NO.[33] Dissociation of NO_2 has precedent in a recent flash photolysis study[34] where it was shown that the manganese(III) nitrito complex Mn(TPP)(ONO) undergoes metal−oxygen homolysis as its principal photoreaction pathway. The O−NO bond cleavage reported earlier for this system is apparently a much lower yield primary photoreaction.

At first glance, such a circuitous route to regenerate Ru(P)(NO)(ONO) would seem unlikely, given what appeared to be the direct regeneration of this species by reaction of **B** with NO. However, a stopped flow kinetics study in this laboratory has identified $Ru(TmTP)(NO)_2$ as a key reactive intermediate in the mechanism by which Ru(TmTP)(CO) reacts with NO to give **3**.[11b] Under excess NO, this species undergoes a relatively slow reaction by a step second-order in [NO] to give **3** plus N_2O (eq 9). $Ru(TmTP)(NO)_2$ and Ru(TmTP)(NO)(ONO) have

$$Ru^{II}(TmTP)(CO) \overset{+2NO,\ -CO}{\rightleftharpoons} Ru^{II}(TmTP)(NO)_2 \xrightarrow{+2NO} \mathbf{3} + N_2O \quad (9)$$

similar spectra in the Soret region, both displaying λ_{max} at 411 nm, although the former displays a somewhat lower extinction coefficient at the λ_{max} and a somewhat broader band.[11b] The spectral differences in the Q-band region are somewhat larger. *As noted above*, residual, much longer lived, absorbance differences remained after the $k_A(i)$ and $k_B(i)$ pathways had run their course. Qualitatively, these residual spectra are consistent with the difference spectrum between $Ru(TmTP)(NO)_2$ and **3**. Furthermore, the slow reactions under NO to regenerate **3** are consistent with the kinetics of $Ru(TmTP)(NO)_2$ oxidation by NO studied in this laboratory.[11b]

Isotopic Exchange Experiments. Neither the transient spectra nor the reaction kinetics differentiate satisfactorily between the alternatives described in Schemes 2 and 3 for the formation of **B**(*i*). For this reason, we examined the photoreactions in the presence of the fully isotopically labeled nitric oxide $^{15}N^{18}O$. Figure 6a compares the FTIR spectra of Ru(TmTP)(NO)(ONO) (**3**) in methylcyclohexane-d_{14} (MCH-d_{14}, which has an appropriate IR window) with the fully labeled analogue $Ru(TmTP)(^{15}N^{18}O)(^{18}O^{15}N^{18}O)$ prepared as described in the Experimental Section. The key features are the shift of the ν_{NO} band from 1841 to 1763 cm^{-1} and the shift of the asymmetric stretch of coordinated nitrite ion (ν_{ONO}) from 1526 to 1460 cm^{-1}. The ratio of peak heights $Abs(\nu_{NO})/Abs(\nu_{ONO})$ is 4.2 (±0.2) for each compound. Figure 6b displays the temporal FTIR spectra, presented in the ΔAbs format, after a deoxygenated solution of **3** (about 3 mM) has been subjected to near UV irradiation under an atmosphere of $^{15}N^{18}O$ (about 5 mM). In each case, the time between the photolysis event and recording the FTIR spectrum was several minutes. Over the experiment time frame, thermal reactions were minimal, but upon photolysis, isotopic labels were incorporated into **3** as evidenced by the net depletion of both the ν_{NO} and ν_{ONO} peaks corresponding to the unlabeled compound and the growth of new peaks at 1805, 1765, 1500, and 1462 cm^{-1}. (Analogous photolysis of **3** under normally labeled NO leads to little change in the IR spectrum.) There were no changes in the optical absorption bands. It is clear from these spectral data *that isotopic labeling from the $^{15}N^{18}O$ is being incorporated into both the nitrosyl and the nitrito ligands of **3** as a consequence of the photolysis*.

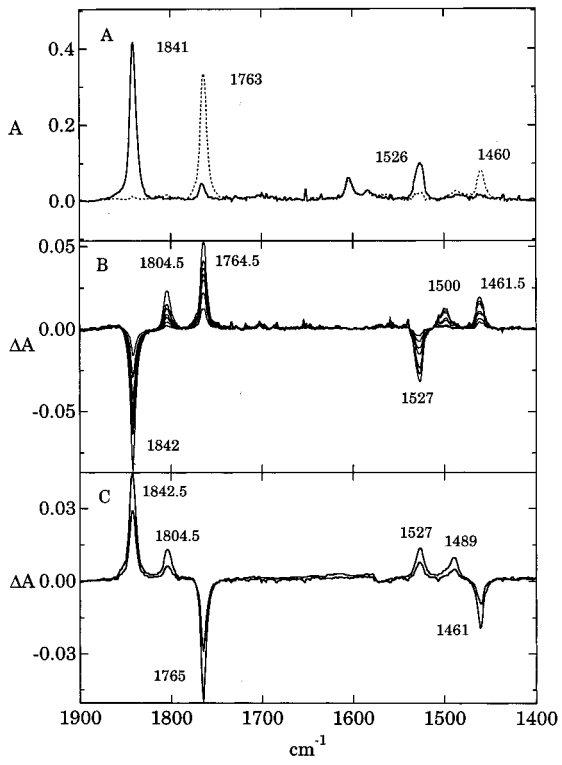

Figure 6. (a) IR spectra of the Ru(TmTP)(NO)(ONO) and Ru(TmTP)($^{15}N^{10}O$)($^{18}O^{15}N^{18}O$) in perdeuteriomethylcyclohexane. (b) Difference spectrum for the 365 nm photolysis of Ru(TmTP)(NO)(ONO) (∼3 mM) under $^{15}N^{18}O$ (∼5 mM) in cyclohexane. Spectra were taken after 0.5, 1.0, 1.5, 2.0, 2.5, 3.0, and 4.0 min of photolysis. (c) Difference spectrum for the 365 nm photolysis of Ru(TmTP)($^{15}N^{18}O$)($^{18}O^{15}N^{18}O$) (∼3 mM) under NO (∼5 mM) in cyclohexane solution. Spectra were taken after 1.0 and 2.0 min of photolysis.

In Figure 6b, the sum of the absorbance changes for the 1805 and 1765 cm^{-1} peaks (ΔAbs_{1805} plus ΔAbs_{1765} values) is nearly identical to the decreased absorbance at 1842 cm^{-1} ($-\Delta Abs_{1842}$), and the sum of ΔAbs_{1500} plus ΔAbs_{1462} nearly equals $-\Delta Abs_{1526}$. These results suggest that isotopically labeled **3** is the only observable photoproduct several minutes after the continuous photolysis experiment. *That is, any primary photoreactions leading to labilization or reaction of either the nitrosyl or nitrito ligands are reversible.* However, the ratio of the negative peaks corresponding to depletion of normally labeled **3** ($\Delta Abs_{1842}/\Delta Abs_{1562}$) is 2.8 ± 0.2, less than the peak height ratio (4.2) noted above for the spectrum of normally labeled **3** in Figure 6a. If we assume Scheme 2 to be in effect, i.e., that the exchange of $^{15}N^{18}O$ into the respective coordinated nitrosyl and nitrito ligands are independent photochemical events, the proportionally greater change at 1526 cm^{-1} would indicate a ∼50% larger quantum yield for NO labilization from Ru−ONO than from Ru−NO. On the other hand, if Scheme 3 were in effect, there would be a second pathway for exchange of the Ru(NO) nitrosyl. Reaction of $^{15}N^{18}O$ with Ru(TmTP)(NO) would give Ru(TmTP)(NO)($^{15}N^{18}O$), and this could undergo further reaction with $^{15}N^{18}O$, leading to oxidation of either nitrosyl to nitrite. Oxidation of the unlabeled NO would give

(32) Scheidt, W. R.; Frisse, M. E. *J. Am. Chem. Soc.* **1975**, *97*, 17−20.
(33) Graetzel, M.; Taniguchi, S.; Henglein, A. *Ber. Bunsen-Ges. Phys. Chem.* **1970,** *74*, 488−492.
(34) Hoshino, M.; Nagashima, Y.; Seki. H.; DeLeo, M.; Ford, P. C. *Inorg. Chem.* **1998,** *37*, 2464−2469.

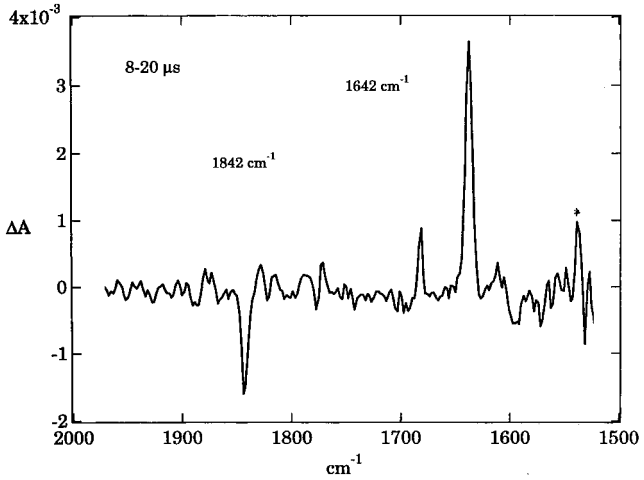

Figure 7. Step-scan FTIR spectrum of a solution of **3** in cyclohexane during the 8−20 μs window after 355 nm laser excitation.

a nitrite with a single ^{18}O incorporated plus a fully labeled nitrosyl, i.e., Ru(TmTP)($^{15}N^{18}O$)(O$^{15}N^{18}O$); on the other hand, $^{15}N^{18}O$ oxidation of coordinated $^{15}N^{18}O$ would give fully labeled nitrite and unlabeled nitrosyl, i.e., Ru(TmTP)(NO)($^{18}O^{15}N^{18}O$). The former process, although occurring through photoactivation of the coordinated nitrite, effectively leads to exchange of $^{15}N^{18}O$ for NO. If all such exchange were via this pathway, the $\Delta Abs_{1842}/\Delta Abs_{1526}$ ratio of the negative peaks in Figure 7b should be ~2.1 (half the 4.2 noted for Figure 6a). The larger value of 2.8 confirms the conclusion that, regardless of the pathway for nitrite activation, there must also be an independent direct photolabilization of NO to give **A**(**3**).

The formation of the two (labeled) nitrite bands at 1462 and 1500 cm^{-1} in Figure 7b is consistent with the fully labeled and partially labeled nitrite complexes predicted by Scheme 3. However, the peaks appear at somewhat uneven intensities, the band at 1462 cm^{-1} appearing ~50% more intense. An unknown in this analysis is the ν_{ONO} band maximum for the doubly labeled nitrite coordinated at the nonenriched oxygen Ru(P)(NO)-(O$^{15}N^{18}O$), i.e., the product predicted for $^{15}N^{18}O$ reaction with the O═Ru(P)(NO) of Scheme 2. While we expect this to appear at a frequency higher than for the fully labeled nitrite complex, the ν_{ONO} frequency might be sufficiently localized to the NO double bond that the isotopic mass of the metal-coordinated oxygen would not measurably affect it. If so, the somewhat higher intensity of the 1462 cm^{-1} band might be reflective of a modest contribution from Scheme 2.

A somewhat more puzzling observation in Figure 6b is the appearance of the band at 1805 cm^{-1}. This appears only in the presence of labeled NO, and the summed intensities of the bands at 1805 and 1765 cm^{-1} equal the negative peak at 1842 cm^{-1}; thus, we conclude that this band represents the ν_{NO} of a monosubstituted nitrosyl, probably Ru−^{15}NO. At the longer irradiation times, the Abs_{1765}/Abs_{1805} ratio is ~3, but at earlier photolysis times, the ratio is larger, indicating that the two are not formed by competitive reactions from a common intermediate. We suspect a secondary photoreaction but cannot offer an obvious mechanism for this process.

Further evidence for NO_2 loss as a major photochemical pathway for **3** is provided by the complementary experiment to Figure 6b, i.e., photolysis of fully labeled **3** in the presence of unlabeled NO. Notably, unlabeled nitrito ligand was formed as a photoproduct as predicted by Scheme 3. Also if Ru-(TmTP)(NO)($^{15}N^{18}O$) were indeed an intermediate, a doubly labeled nitrite would also be predicted as a product. The peak in Figure 6c at 1489 cm^{-1}, 11 cm^{-1} lower than the mixed labeled nitrite peak in Figure 6b, suggests a doubly labeled nitrite, as predicted.

Time-Resolved Infrared Studies. Attempts to identify the various transients from the differences detected in the Soret band and Q-band regions of the electronic spectra are frustrated by the strongly overlapping nature of these bands. However, the presence of a strong IR chromophore such as coordinated NO might be exploited in trying to identify intermediates using TRIR. In this context, preliminary experiments were initiated to probe possible IR detectable species in the 355 nm flash photolysis of **3** in cyclohexane solution using the step-scan FTIR instrumentation at Los Alamos National Laboratory.[19] These studies, which pushed the limits of detection, clearly demonstrated bleaching of the strong 1842 cm^{-1} ν_{NO} band (S/N ≈ 3) characteristic of **3** and the appearance of a new, stronger band at 1642 cm^{-1} (S/N ≈ 7), which was longer lived than the maximum time frame of the instrument (240 μs) even in the presence of 5 mM NO (Figure 7). Examining the dynamic absorbance changes at 1642 cm^{-1} in the 1−10 μs time frame suggested that this has a rise time of ~5 μs ($k_{obs} \approx 2 \times 10^5$ s^{-1}) which, assuming linear dependence on [NO], would give a second-order rate constant of 4×10^7 M^{-1}s^{-1}. Notably, this value is comparable to the value of k_B(**3**) ($(4.5 \pm 0.7) \times 10^7$ M^{-1}s^{-1}) determined in benzene. Thus, while the slower decay process was not seen at the wavelengths probed in the TRO studies of the flash photolysis of **3** in cyclohexane, it appears to be clearly identifiable in the TRIR studies. Furthermore, the long-lived (τ > 1 ms) ν_{NO} absorption at 1642 cm^{-1} is consistent with the residual optical spectrum, suggesting the presence of Ru(TmTP)$(NO)_2$. One might have expected a second, higher frequency ν_{NO} band for this species (which might be formulated as Ru^{II}(TmTP)(NO^+)(NO^-)), but if weaker, this might have been obscured by the relatively low signal-to-noise ratio (S/N) of the experiments. Nonetheless, we view these data as supporting the role of Scheme 3 in the photoactivation of the coordinated nitrite under these conditions.

Summary

The flash photolysis data reported here for the nitrosyl nitrito complexes Ru(P)(NO)(ONO) in hydrocarbon solvents clearly indicate the operation of *at least* two pathways leading to the formation of photoreaction intermediates. One of these is NO photodissociation to give Ru^{III}(P)(ONO) (or its solvated analogue) which decays by a fast second-order reaction with NO to regenerate the starting complex. Support for this pathway comes from the TRO spectral properties of the intermediate **A**(*i*), especially in comparison to spectral properties of intermediates in the flash photolysis of the chloro nitrosyl analogue Ru(P)-(Cl)(NO), and in isotope exchange reactions in the presence of the labeled NO.

A second pathway involves the nitrito ligand, and the cumulative evidence points to this being the result of NO_2 photodissociation to give Ru(P)(NO) which is trapped by the excess NO present to give the very much longer lived dinitrosyl complex Ru(P)$(NO)_2$ (Scheme 3). This species has also been detected in stopped flow spectral experiments studying the reaction of NO with Ru(P)(CO).[11b] The dinitrosyl complex reacts either with the excess NO present or with N_2O_3 to regenerate Ru(P)(NO)(ONO). An alternate pathway for nitrite activation would be the reversible photodissociation of NO from the nitrite to give the nitrosyl oxo complex Ru(P)(NO)(O), but with the exception of possible ambiguity in ratios of isotope exchange products, this mechanism now seems incompatible with the photoreaction data.

Acknowledgment. This work was supported by the National Science Foundation (Grants CHE 9400919 and CHE 9726889) and by a Collaborative UC/Los Alamos Research (CULAR) Initiative grant from Los Alamos National Laboratory. TRO experiments were carried out on systems constructed with instrumentation grants from the U.S. Department of Energy University Research Instrumentation Grant Program (No. DE-FG-05-91ER79039) and from the National Science Foundation. S.B. thanks the Swiss National Science Foundation for a Postdoctoral Fellowship. We are also grateful to Professors K. Kadish (University of Houston) and G. Richter-Addo (University of Oklahoma) for providing a copy of ref 26 before publication and to Professor D. S. Bohle (University of Wyoming) for providing a copy of ref 13a before publication. Professor Bohle also supplied several compounds, which, while not used in this study, provided insight into properties of ruthenium porphyrin nitrosyl complexes.

JA981907O